

See discussions, stats, and author profiles for this publication at: <https://www.researchgate.net/publication/269412791>

Jatrophanes from Euphorbia squamosa as Potent Inhibitors of Candida albicans Multidrug Transporters

ARTICLE in JOURNAL OF NATURAL PRODUCTS · DECEMBER 2014

Impact Factor: 3.8 · DOI: 10.1021/np500756z · Source: PubMed

CITATION

1

READS

114

8 AUTHORS, INCLUDING:



Yalda Shokoohinia

Kermanshah University of Medical Sciences

37 PUBLICATIONS 172 CITATIONS

SEE PROFILE



Behzad Zolfaghari

Isfahan University of Medical Sciences

68 PUBLICATIONS 478 CITATIONS

SEE PROFILE



Orazio Taglialatela-Scafati

University of Naples Federico II

166 PUBLICATIONS 2,353 CITATIONS

SEE PROFILE



Attilio Di Pietro

Institute for the Biology and Chemistry of Pr...

174 PUBLICATIONS 4,216 CITATIONS

SEE PROFILE

Jatrophanes from *Euphorbia squamosa* as Potent Inhibitors of *Candida albicans* Multidrug Transporters

Manpreet Kaur Rawal,[†] Yalda Shokoohinia,[‡] Giuseppina Chianese,[§] Behzad Zolfaghari,[⊥] Giovanni Appendino,^{||} Orazio Taglialatela-Scafati,^{*,§} Rajendra Prasad,^{†,⊗} and Attilio Di Pietro^{*,∇,⊗}

[†]School of Life Sciences, Jawaharlal Nehru University, 110067 New Delhi, India

[‡]Department of Pharmacognosy and Biotechnology, School of Pharmacy, Kermanshah University of Medical Sciences, 6734667149 Kermanshah, Iran

[§]Dipartimento di Farmacia, Università di Napoli Federico II, Via Montesano 49, 80131 Naples, Italy

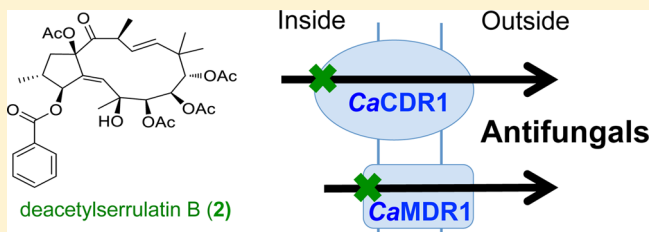
[⊥]Department of Pharmacognosy, School of Pharmacy, Isfahan University of Medical Sciences, 84156-83111 Isfahan, Iran

^{||}Dipartimento di Scienze del Farmaco, Università del Piemonte Orientale, Via Bovio 6, 28100 Novara, Italy

[∇]Equipe Labellisée Ligue 2014, BMSS UMR5086 CNRS, University of Lyon, IBCP, Passage du Vercors 7, 69367 Lyon, France

Supporting Information

ABSTRACT: A series of structurally related jatrophone diterpenoids (1–6), including the new euphosquamosins A–C (4–6), was purified from the Iranian spurge *Euphorbia squamosa* and evaluated for their capacity to inhibit drug efflux by multidrug transporters of *Candida albicans*. Three of these compounds showed an interesting profile of activity. In particular, deacetylserriatin B (2) and euphosquamosin C (6) strongly inhibited the drug-efflux activity of the primary ABC-transporter CaCdr1p, an effect that translated, in a yeast strain overexpressing this transporter, into an increased sensitivity to fluconazole. These compounds were transported by CaCdr1p, as shown by the observation of an 11–14-fold cross-resistance of yeast growth, and could also inhibit the secondary MFS-transporter CaMdr1p. In contrast, euphosquamosin A (4) was selective for CaCdr1p, possibly as a result of a different binding mode. Taken together, these observations suggest jatrophone diterpenes to be a new class of potent inhibitors of multidrug transporters critical for drug resistance in pathogenic yeasts.



Transplantation surgery, cancer chemotherapy, and HIV infections have led to a worldwide rise of the immunocompromised population, and hence also of bacterial and fungal opportunistic infections.¹ The fungal genera most often associated with invasive fungal infections include *Candida*, *Aspergillus*, and *Cryptococcus*,² with opportunistic strains of *Candida albicans* accounting for approximately 50–60% causes of candidiasis, particularly in immunocompromised patients. The treatment of these *Candida* infections relies heavily on azole antifungal agents,³ for which the widespread and prolonged use has led to the rapid emergence of multidrug resistant (MDR) isolates of *C. albicans* as well as of non-*albicans* species.⁴ Various mechanisms potentially contributing to the development of MDR have been identified, and the induction of genes encoding drug-efflux pumps, like the ATP-binding cassette (ABC) transporters genes *CaCDR1* and *CaCDR2* and the major-facilitator superfamily (MFS) transporter gene *CaMDR1*, has been shown to play a prominent role in the development of resistance to antifungal drugs.^{5–7} Overexpression of these pump proteins may lead to an increased efflux of drug substrates in MDR clinical isolates.^{4,8}

A search for novel inhibitors capable of blocking the drug extrusion mediated by these efflux proteins represents an

attractive approach to reverse MDR, intensely pursued by 50 decades for ABC transporters of relevance in cancer research, 51 but still in its infancy for those involved in drug resistance in 52 pathogenic yeasts. The synthetic D-octapeptide KN20⁹ and 53 various microbial natural products, exemplified by enniatins, 54 tacrolimus/FK506, unnarmicins, and milbemycins,^{10–14} were 55 found to modulate drug efflux by inhibiting fungal multidrug 56 transporters. However, these compounds display a pleiotropic 57 profile of bioactivity, modulating a host activity and other 58 targets, as do the synthetic agent disulfiram (Antabuse) and the 59 plant natural products curcumin, a multifunctional diaryl- 60 heptanoid, and farnesol, a skin-allergenic sesquiterpene.^{15–17} 61

Some macrocyclic diterpenoids from Euphorbiaceae plant species are potent inhibitors of the human P-glycoprotein 62 transporter. These include lathyranes from *Euphorbia lathyris* 63 L.^{18,19} and *E. lagascae* Spreng.,²⁰ jatrophanes from *E. dendroides* 64 L.²¹ *E. peplus* L.²² and *E. esula* L.,²³ and both lathyranes and 65 jatrophanes from *Euphorbia helioscopia* L.²⁴ Based on the 66 availability of these compounds, the design of a rudimental 67 pharmacophore has been proposed.^{25,26} Evidence is currently 68 69

Received: September 26, 2014

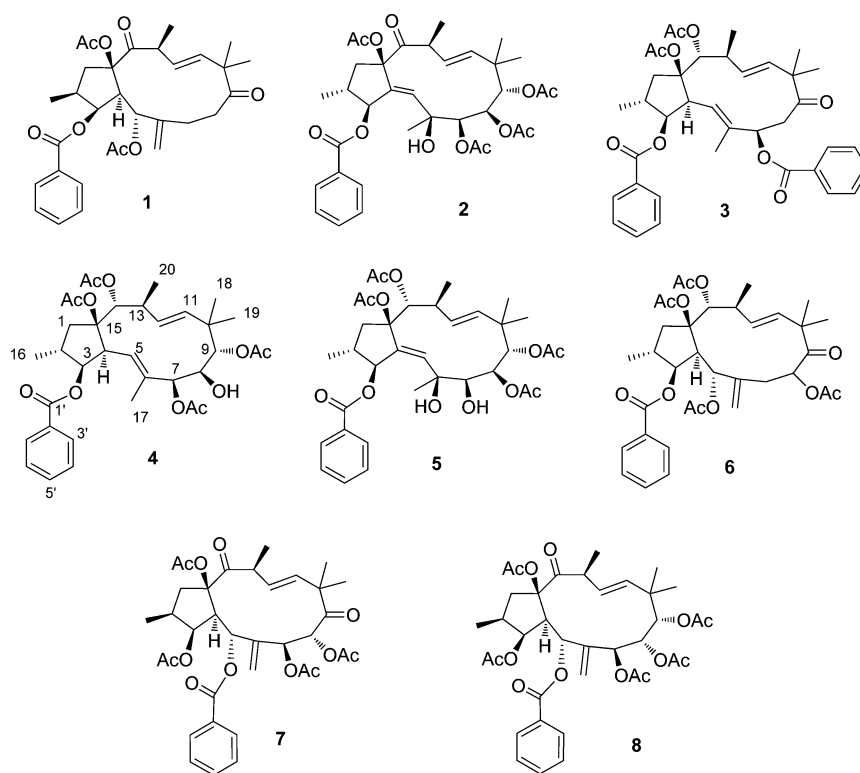


Figure 1. Chemical structures of compounds studied: compounds 1–6 were isolated in the present study, and the structurally related compounds 7 and 8 were obtained previously from *Euphorbia bungei* Boiss.³⁰

presented that some jatrophanes from the Iranian spurge *Euphorbia squamosa* Willd. are potent inhibitors of yeast *CaCdr1p* and *CaMdr1p*, sensitizing yeast growth at sub-micromolar concentrations in the presence of fluconazole (FLC). Some structural features crucial for this pharmacological activity have also been identified. To our knowledge, this is the first report on the chemical composition of *Euphorbia squamosa*.

RESULTS AND DISCUSSION

Compound Purification and Characterization. Dried aerial parts of *E. squamosa* were extracted exhaustively with acetone at room temperature. The depigmented (lead acetate) extract was filtered on Celite and then partitioned between aqueous ethanol and CH_2Cl_2 . Fractionation of the less polar phase by column chromatography on silica gel, followed by HPLC, led to the isolation of six polyacyl jatrophane diterpenoids. Three of them [guyonianin B (1),²⁷ deacetyl-serrulatin B (2),²⁸ and euphoscopin C (3)²⁹] were identified by comparing their spectroscopic data with those reported in the literature,^{27–29} while 4–6 (euphosquamosins A–C) are new (Figure 1).

Euphosquamosin A (4) was isolated as a colorless amorphous solid with the molecular formula $\text{C}_{35}\text{H}_{46}\text{O}_{11}$ (HRESIMS). Inspection of the ^{13}C NMR spectrum of 4 (CDCl_3) disclosed the presence of five ester carbonyls (δ_{C} 171.3, 170.4, 169.4, 169.3, 166.0), a phenyl ring, and four additional sp^2 carbons; thus, to account for the two remaining unsaturation degrees implied in the molecular formula, compound 4 must be bicyclic. Analysis of the ^1H and ^{13}C NMR data of 4 strongly suggested the molecular architecture of a penta-esterified diterpenoid of the jatrophane family. The five acylating groups were identified as four acetates and one

benzoate on the basis of characteristic signals in the ^1H and ^{13}C NMR spectra.

The resonances of the diterpenoid core of 4 were analyzed with the help of 2D-NMR experiments; in particular, the COSY spectrum revealed the existence of three distinct spin systems, as shown in bold in Figure 2. The first one (A) spanned from

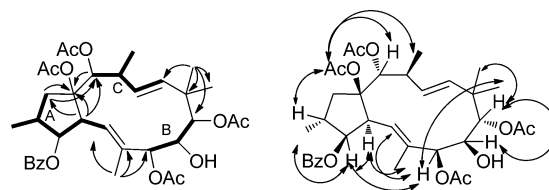


Figure 2. Diagnostic 2D-NMR correlations of 4. Left, COSY (bold) and HMBC (arrows); right, ROESY.

$\text{H}_2\text{-1}$ to the vinylic H-5 through the methyl-branched C-2 and the oxymethine C-3 . The second (B) included three consecutive oxymethines (H-7 to H-9), while the third (C) spanned from the *trans* *vic*-disubstituted double bond H-11/H-12 ($J = 16.0$ Hz) to the oxymethine H-14 and included the methyl-branched methine at C-13 . All the proton resonances were associated with those of the relevant carbon atoms by the HSQC spectrum and, then, the $^2,3J_{\text{H,C}}$ HMBC spectrum was used to link the three moieties to quaternary carbons and tertiary methyls, as shown in Figure 2. HMBC correlations shown between $\text{H}_3\text{-17}$ and $\text{H}_3\text{-18/H}_3\text{-19}$ were used to join moieties A with B, and B with C, respectively, while the correlations of $\text{H}_2\text{-1}$ with C-14 and of both $\text{H}_2\text{-1}$ and H-14 with the non-protonated oxygenated C-15 (δ_{C} 93.5), were used to establish this latter carbon as the connection point between fragments A and C. Finally, HMBC correlations of H-4 with C-12

1, C-14, and C-15 defined unambiguously the bicyclic architecture of euphosquamosin A. The jatrophane core of **4** was found to include six oxygenated sp^3 carbons (C-3, C-7, C-8, C-9, C-14, C-15), of which five were esterified. The HMBC cross-peak of H-3 with the ester carbonyl at δ_C 166.0 was used to locate the benzoyl group at C-3, and, similarly, three of the four acetyl groups could be located at C-7, C-9, and C-14. The relatively high-field H/C resonances for the oxymethine at C-8 (δ_H 3.74; δ_C 68.3) and the relatively low-field-shifted resonance of C-15 suggested the placement of the fourth acetyl group at this latter position. The relative configuration of the stereogenic centers of **4** was deduced from the network of cross-peaks present in the 2D ROESY spectrum, partly reported in Figure 2B, and by comparison with literature data.³⁰ The *E* configuration of the endocyclic double bond was indicated by the ROESY cross-peaks H-5/H-7 and H₃-17/H-4; the proton at the ring junction (H-4) displayed also ROESY correlations with H₃-16 and H-7 indicating the *cis* (conventionally α) orientation of these protons. The ROESY cross-peak of the acetoxy methyl at C-15 with H-2, H-14, and H₃-20 revealed their β -orientation, while the additional diagnostic ROESY correlations of H₃-18 with H-7 and H-8, and of H₃-19 with H-9 allowed the complete definition of the relative stereostructure of euphosquamosin A (**4**). Taking advantage of the presence of a free secondary hydroxy group in the structure of **4**, the absolute configuration was determined using Mosher's method.³¹ Thus, **4** was independently treated with (–)- and (+)- α -methoxy- α -(trifluoromethyl)phenylacetic acid (MTPA) chloride in dry pyridine, affording the corresponding S-(**4a**) and R-(**4b**) MTPA ester derivatives, respectively. The distribution of $\Delta\delta$ (S–R) values (Figure 3), reflecting the anisotropic effect of MTPA according to the Mosher's model,³¹ indicated an 8S configuration.

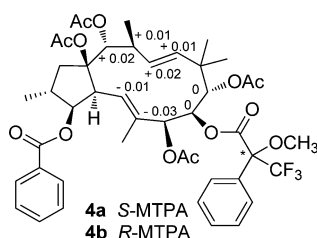


Figure 3. MTPA derivatives of euphosquamosin A (**4**), with $\Delta\delta_{(S-R)}$ values in ppm.

Euphosquamosin B (**5**) was assigned the molecular formula $C_{35}H_{46}O_{12}$, with one additional oxygen atom compared to **4**, by HRESIMS. The ¹H and ¹³C NMR data of **5** were analyzed by 2D-NMR spectroscopy, following the same approach as detailed above for **4**. This analysis located the differences between euphosquamosins A (**4**) and B (**5**) at the “southern” part of the molecule, namely, in the sequence C-4 to C-8. In particular, a carbon–carbon double bond at $\Delta^{4(5)}$, instead of Δ^5 , well explained the low-field resonance of H-5 (δ_H 6.72, s) and the downfield shift of H-3 (from δ_H 4.96 to 6.35). The additional oxygen atom implied by the molecular formula should be attached at the unprotonated sp^3 carbon C-6 resonating at δ_C 78.1. The HMBC cross-peaks of H₃-17 with C-5, C-6, and C-7 and of H-3 with C-4, C-5, and C-15 further confirmed this substructure. The HMBC spectrum was also

instrumental in locating the benzoyl group at C-3 and three acetyl groups at C-8, C-9, and C-15, respectively, while the relatively high field resonance of H-7 (δ_H 3.42) indicated the presence of a non-acylated hydroxy group at C-7. Thus, the fourth acetyl group could be attached either at the quaternary carbon C-15 or C-6. Its placement at C-15 was based mainly on the comparison of ¹³C NMR resonances of **5** with those of **3** and **4** and from the ROESY cross-peaks observed. Indeed, OAc-15 showed ROESY correlations with H-2, H-14, and H₃-20, also indicating the relative configuration in the “northern” part of the molecule. The ROESY correlations of H₃-18 with H-7 and H-8, of H₃-19 with H-9, and of H₃-17 with H-8 and H-3 defined the relative configuration of the four consecutive oxygenated sp^3 carbons and the *E* configuration at the trisubstituted double bond, thus completing the relative stereostructure of euphosquamosin B (**5**).

HRESIMS analysis assigned the $C_{35}H_{44}O_{11}$ molecular formula to euphosquamosin C (**6**), implying one additional unsaturation when compared to **4**. The ¹H NMR spectrum of **6** showed clearly the presence of one benzoyl and four acetyl groups, one *vic*- and one *gem*-disubstituted double bond (δ_H 4.60 and 4.39, both bs), and four methyl groups (two doublets and two singlets). All the ¹H NMR signals of **6** were associated with those of directly attached carbon atoms through the HSQC experiment, thus disclosing the presence of four oxymethines. Notably, the ¹³C NMR spectrum of **6** revealed the presence of a ketone carbonyl (δ_C 210.3) and of a further quaternary oxygenated sp^3 carbon (δ_C 87.9).

A thorough investigation of the 1D- and 2D-NMR spectra of **6** revealed that, just like with **5**, the structural moieties C-1 to C-4 and C-10 to C-15 were superimposable on those of euphosquamosin A (**4**), indicating the same relative configuration. Therefore, the structural differences between **4** and **6** could be located in the region spanning from C-5 to C-9. The COSY spectrum revealed the vicinal coupling of H-4 with the oxymethine H-5 and of the diastereotopic methylene H₂-7 with the oxymethine H-8. The HMBC correlations of the *exo*-methylene H₂-17 with C-5 (δ_C 70.2), C-6 (δ_C 139.2), and C-7 (δ_C 34.3), and those of both H₃-18 and H₃-19 with the ketone carbonyl (C-9), were used to define the location of the functional groups around the jatrophane core of **6**. Since the benzoyl group was attached at O-3 on the basis of HMBC cross-peak between H-3 and the ester carbonyl, the remaining four oxygenated sp^3 carbons must be all acetylated. The ROESY correlations of H-2 with both OAc-15 and OAc-5 suggested the relative configuration at C-5, although, unfortunately, no diagnostic ROESY cross-peak was exhibited by H-8 and OAc-8. Therefore, the configuration at this center has been left unassigned.

Inhibition of *Candida albicans* Multidrug Transporters. All the jatrophane derivatives obtained (**1**–**6**) were assayed for their ability to inhibit drug-efflux activity of the two multidrug transporters of *C. albicans*, CaCdr1p and CaMdr1p, overexpressed in a *Saccharomyces cerevisiae* strain deleted from its own multidrug transporters. To increase the chemical diversity of the compounds tested, the structurally related compounds **7** and **8** (Figure 1), recently obtained from *Euphorbia bungei* Boiss were also evaluated.³⁰ Figure 4A shows that about half of the compounds inhibited the CaCdr1p-mediated efflux of Nile Red (NR), according to the following order of efficiency: **2** > **6** > **4** > **1**, with **2** showing a marked inhibition (88%) higher than that of the reference curcumin (CUR) against rhodamine 6G (R6G) efflux. Despite their

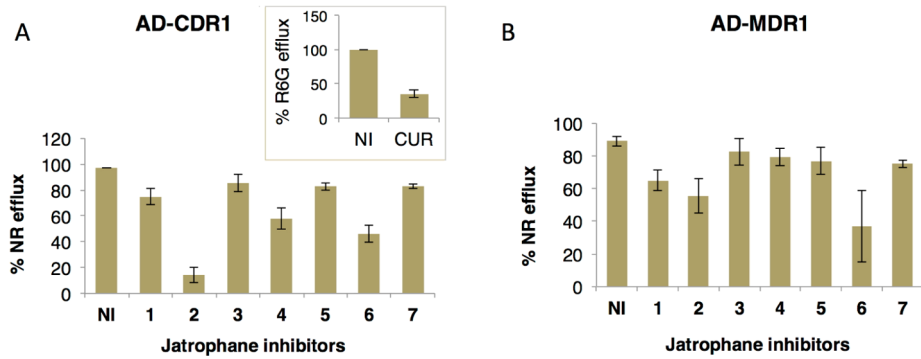


Figure 4. Effects of jatrophane inhibitors (1–7) on Nile Red (NR) efflux by *CaCdr1p* and *CaMdr1p*. *S. cerevisiae* cells overexpressing the *CaCdr1p* ABC-transporter (AD-CDR1) (A) and the *CaMdr1p* MFS-transporter (AD-MDR1) (B) were incubated with 7 μ M NR in the presence of 10-fold excess of each jatrophane inhibitor or no inhibitor (NI). Values are the means \pm standard deviations (error bars) for three independent experiments. Compound 8, which was earlier found to be devoid of any inhibitory activity, is not represented here. Inset shows inhibition of rhodamine 6G (R6G) efflux in the presence of curcumin (CUR) taken as a positive control for *CaCdr1p* inhibition.

Table 1. Intrinsic Cytotoxicity of Jatrophane Inhibitors

yeast strain	2		4		6	
	IC ₅₀ (μ M) ^a	RI ^b	IC ₅₀ (μ M) ^a	RI ^b	IC ₅₀ (μ M) ^a	RI ^b
AD1-8u [−]	2.3 \pm 0.3	1.0	2.3 \pm 0.3	1.0	2.3 \pm 0.3	1.0
AD-CDR1	26.7 \pm 2.9**	11.6	3.7 \pm 1.2	1.6	31.7 \pm 2.9**	13.8
AD-MDR1	28.3 \pm 2.9**	12.3	3.5 \pm 1.3	1.5	25.0 \pm 5.0**	10.9

^aThe IC₅₀ values of cytotoxicity were determined by measuring optical density of each strain in the absence and presence of a range of concentrations of the different jatrophanes tested. Yeast growth in the absence of inhibitor was considered as 100%, and the concentration where growth was decreased to 50% was taken as IC₅₀. ^bThe resistance index (RI) was calculated as the ratio between the IC₅₀ values determined for the strain overexpressing either *Cdr1p* (AD-CDR1) or *Mdr1p* (AD-MDR1) relative to that of the control strain (AD1-8u[−]). The values are the means \pm standard deviations of three independent experiments. Differences between the means were analyzed by the Student's *t*-test; they were statistically significant when indicated (***p* \leq 0.05).

Table 2. Ability of Jatrophane Inhibitors To Sensitize Yeast Growth to FLC Cytotoxicity^a

strain	inhibitor	FIC of FLC	FIC of inhibitor	FICI
AD1-8u [−]	2	1.2 (1.5/1.25)	0.07 (0.15/2.3)	1.27 (1.2 + 0.07)
	4	1.2 (1.5/1.25)	0.07 (0.15/2.3)	1.27 (1.2 + 0.07)
	6	1.2 (1.5/1.25)	0.07 (0.15/2.3)	1.27 (1.2 + 0.07)
AD-CDR1	2	0.02 (3.12/150)	0.01 (0.31/26.7)	0.03 ^b (0.02 + 0.01)
	4	0.08 (12.5/150)	0.34 (1.25/3.7)	0.42 ^b (0.08 + 0.34)
	6	0.04 (6.25/150)	0.02 (0.62/31.7)	0.06 ^b (0.04 + 0.02)
AD-MDR1	2	0.5 (6.25/12.5)	0.02 (0.62/28.3)	0.52 ^b (0.50 + 0.02)
	4	1.0 (12.5/12.5)	0.36 (1.25/3.5)	1.36 (1.0 + 0.36)
	6	1.0 (12.5/12.5)	0.02 (0.62/25)	1.02 (1.0 + 0.02)

^aEvaluated by the checkerboard method recommended by the Clinical and Laboratory Standards Institute (CLSI) and expressed as the fractional inhibitory concentration (FIC) values for the FLC substrate (= IC₅₀ of FLC in combination/IC₅₀ of FLC alone) and each jatrophane inhibitor (= IC₅₀ of inhibitor in combination/IC₅₀ of inhibitor alone). ^bA FIC index (FICI) value \leq 0.5 indicates synergistic interaction between the inhibitor and the substrate.

apparent close structural similarity with 2, compounds 3, 5, and 7, as well as 8, produced no significant inhibition. Since compounds 1–6 are very similar in the five-membered A-ring, the marked differences observed in the inhibitory activity could be attributed to the functionalization of the macrocyclic B-ring. Since the structurally related compounds investigated displayed multiple differences, it was difficult to propose structure–activity relationships at a precise pharmacophore. Remarkably, jatrophanes from the same series also inhibited the drug-efflux activity of *CaMdr1p* (Figure 4B), but with different efficiency and, surprisingly, different structure–activity relationships. Indeed, when compared to *CaCdr1p*, the order of

efficiency seems different, with 4 showing very low activity and compound 2 showing almost the same efficiency as 1. Thus, while 2 and 6 behaved as dual inhibitors, producing strong interactions with both types of multidrug transporters, 4 selectively inhibited *CaCdr1p*. When assayed for cytotoxicity, the three most efficient *CaCdr1p* inhibitors displayed IC₅₀ values for the control yeast cells AD1-8u[−] of 2.3 μ M (Table 1). The two dual inhibitors, 2 and 6, were much less cytotoxic for the strains overexpressing either *CaCdr1p* or *CaMdr1p*, with IC₅₀ values in the 25.0–31.7 μ M range, corresponding to resistance index (RI) values ranging from 10.9 to 13.8. This transporter-dependent cross-resistance suggests that 2 and 6

might be themselves transported.³² In contrast, compound 4 gave low IC₅₀ values, not significantly different from that of the control cells; such a lack of cross-resistance, with RI values close to unity, suggested the inability of the inhibitor to be transported.

The capacity of the three best inhibitors to sensitize yeast growth to the antifungal activity of FLC is detailed in Table 2. The very low values (0.02–0.08) of fractional inhibitory concentration (FIC) for the FLC substrate observed for all three jatrophone inhibitors in the Cdr1p-overexpressing strain indicated a high capacity of each inhibitor to revert Cdr1p-mediated resistance to FLC. Since the FIC for the inhibitors was also quite low (0.01–0.34), the resulting low values of FICI indicated a strongly synergistic interaction between FLC and both 2 (0.03) and 6 (0.04), whereas a moderate effect was observed with 4 (0.42). This contrasted with the high FICI value (1.27) obtained with the Cdr1p-free control strain, AD1-8u[−], where the inhibitors did not show any effect, as monitored by a high FIC value for FLC (1.2). The high efficiency of 2 toward sensitization to FLC was very similar to that of curcumin (CUR) toward sensitization to rhodamine 6G (R6G, not shown here). The ability of inhibitors to sensitize the growth of the AD-MDR1 yeast strain overexpressing the MFS Mdr1p-transporter was much lower than for the ABC Cdr1p-transporter: only a moderate synergy was observed with 2 (FICI = 0.52), whereas high values (≥1.0) were obtained with the two other inhibitors, 4 and 6. The high value for FIC of FLC (1.0) suggest the inability of the inhibitor to sensitize yeast growth to FLC cytotoxicity. Remarkably, the synergistic interactions between FLC and the active jatrophone derivatives required very low concentrations (0.3–0.6 μM) of the inhibitor.

Jatrophanes from *E. squamosa* as New Inhibitors of Yeast Multidrug Transporters. The high synergism of deacetylerrullatin B (2) at very low concentration (0.3 μM) with FLC toward CaCdr1p indicated a higher efficiency than most previously reported inhibitors (e.g., disulfiram,¹⁵ D-octapeptides,⁹ enniatins,¹⁰ unnarmicins,¹¹ tacrolimus/FK506,¹² curcumin,¹⁶ and milbemycins¹⁴). Deacetylerrullatin B (2) also inhibited the MFS multidrug transporter CaMDR1 and produced a significant synergism with FLC, inducing half reversal at 0.6 μM, and thereby represents one of the most potent inhibitors so far described against CaMdr1p. For comparison, clorgyline, another broad-spectrum inhibitor, required about 10-fold higher concentrations to induce chemosensitization.³³

It is worth mentioning that the inhibition of CaCdr1p by jatrophanes, a class of compounds previously reported to interact with human P-gp,^{18–26} is consistent with the ability of yeast Pdr5p, a *S. cerevisiae* homologue of CaCdr1p, to interact with other types of P-gp inhibitors like some hydrophobic protein kinase C effectors³⁴ and steroids.^{35,36} This might also be related to the observation that, despite the difference in topology between yeast Pdr5p and Cdr1p and human P-gp, all these transporters display widely overlapping panels of substrates^{37,38} mainly constituted by relatively large, unjugated, and highly hydrophobic molecules. This contrasts with the lack of inhibition of CaCdr1p transport activity by known ABCG2-selective inhibitors (R. Prasad and A. Di Pietro, unpublished experiments), despite an overall similar topology, where the transmembrane domain precedes the nucleotide-binding domain in the sequence, by difference with P-gp. This agrees with the observation that macrocyclic diterpenes from *E.*

helioscopia L., which strongly inhibited P-gp, hardly affected ABCG2.²⁴ Such important data should be taken into account for investigating further more potent, and selective CaCdr1p inhibitors. Taken together, these observations qualify macrocyclic jatrophone inhibitors from *E. squamosa* as promising candidates to overcome yeast multidrug resistance associated with the efflux of antifungal drugs, providing a rationale for a systematic investigation of their structure–activity relationships.

EXPERIMENTAL SECTION

General Experimental Procedures. Optical rotations (CHCl₃) were measured at 589 nm on a Perkin-Elmer 192 polarimeter. ¹H (500 MHz), and ¹³C (125 MHz) NMR spectra were measured on a Varian INOVA spectrometer. Chemical shifts were referenced to the residual solvent signal (CDCl₃: δ_H 7.26, δ_C 77.0). Homonuclear ¹H connectivities were determined by the COSY experiment, one-bond heteronuclear ¹H–¹³C connectivities by the HSQC experiment, and two-, and three-bond ¹H–¹³C connectivities by gradient-HMBC experiments optimized for a ²J of 8 Hz. Through-space ¹H connectivities were evidenced by using a ROESY experiment with a mixing time of 500 ms. ESIMS were performed on a LTQ OrbitrapXL (Thermo Scientific) mass spectrometer. Medium-pressure liquid chromatography was performed on a Büchi apparatus using a silica gel (230–400 mesh) column. HPLC were achieved on a Knauer apparatus equipped with a refractive index detector. The Knauer HPLC apparatus was used to assess purity (>95%) of all final products. LUNA (normal phase, SI60, 250 × 4 mm) (Phenomenex) columns were used, eluting with petroleum ether–EtOAc mixtures and 0.7 mL/min as the flow rate.

Plant Material. *Euphorbia squamosa* was collected in the surroundings of Ab-Pari (Mazandaran, Iran) in April 2009. The plant material was identified by Mr. Behram Zehzad, Department of Biology, University of Shaheed Beheshti, and a voucher specimen (No. 2836) has been deposited at the Herbarium of School of Pharmacy, Isfahan University of Medical Sciences, Isfahan, Iran.

Extraction and Isolation. Dried aerial parts (stems, leaves, and flowers) of *E. squamosa* (2.1 kg) were exhaustively extracted with acetone (20 L) at room temperature. After removal of solvent in vacuo, the residue (50 g) was dissolved in ethanol (500 mL), and the same volume of 3% lead acetate was added. After 2 h, the suspension was filtered on a bed of Celite, and the yellowish and clear filtrate was concentrated to remove most of the ethanol and then extracted with CH₂Cl₂. After drying (MgSO₄), the less polar phase was evaporated, affording 6 g of a brown gum. To remove the fatty acids present, the gum was filtered on neutral alumina (60 g) with petroleum ether–EtOAc (4:6) as eluent, eventually affording 2.5 g of a yellowish gum. This was separated by column chromatography (CC) on silica gel with a petroleum ether–EtOAc gradient into ten primary fractions. ¹H NMR analysis of the fractions evidenced the presence of diterpenoids esters in fractions 5–10 (F5–F10). Fraction F5 was purified further by CC on silica gel (petroleum ether–EtOAc gradient, from 9:1 to 7:3) and eventually by HPLC (petroleum ether–EtOAc, 8:2) to afford 3 (9.7 mg ≈ 0.0008%), 5 (12.7 mg ≈ 0.00106%), and 1 (17.4 mg ≈ 0.00145%). Fraction 7 was purified further by gravity column chromatography (CC) on silica gel, first with a petroleum ether–EtOAc gradient, and next with chloroform, eventually yielding 6 (24.7 mg ≈ 0.002%). Fraction F9 was chromatographed on neutral alumina with petroleum ether–EtOAc as eluant and then triturated with ether to afford 100 mg (≈ 0.0083%) of 2. Fraction F10 was purified on silica gel with petroleum ether–EtOAc (7:3) and then subjected to HPLC (petroleum ether–EtOAc, 4:6 as eluant), to afford 4 (21.0 mg ≈ 0.00175%).

Euphosquamosin A (4). Colorless amorphous solid; [α]_D –47 (c 0.5, CHCl₃); ¹H NMR (CDCl₃, 500 MHz) δ 7.93 (2H, d, J = 7.0 Hz, H-3', H-7'), 7.52 (1H, t, J = 7.0 Hz, H-5'), 7.40 (2H, t, J = 7.4 Hz, H-4', H-6'), 5.74 (1H, dd, J = 16.0, 7.5 Hz, H-12), 5.64 (1H, d, J = 10.0 Hz, H-5), 5.08 (1H, d, J = 16.0 Hz, H-11), 4.99 (1H, d, J = 3.0, H-14), 4.96 (1H, m, H-3), 4.95 (1H, bs, H-9), 4.88 (1H, bs, H-7), 3.74 (1H, bs, H-8), 3.47 (1H, dd, J = 14.0, 6.6 Hz, H-1'), 3.27 (1H, dd, J = 10.0, 3.91

392 7.9 Hz, H-4), 2.53 (1H, m, H-13), 2.35 (1H, m, H-2), 2.29 (3H, s, OAc-15), 2.13 (3H, s, OAc-14), 2.07 (3H, s, OAc-9), 1.75 (3H, bs, H-394 17), 1.67 (1H, dd, $J = 14.0, 9.5$ Hz, H-1 α), 1.36 (3H, s, OAc-7), 1.08 (3H, d, $J = 7.0$ Hz, H-16), 1.00 (3H, s, H-18), 0.98 (3H, s, H-19), 0.95 (3H, d, $J = 7.0$ Hz, H-20); ^{13}C NMR (CDCl_3 , 125 MHz) δ 171.3 (s, OAc-14), 170.4 (s, OAc-7), 169.4 (s, OAc-15), 169.3 (s, OAc-9), 166.0 (s, C-1'), 136.4 (d, C-11), 133.4–128.6 (3-OBz 2'-7'), 132.0 (s, C-6), 131.9 (d, C-12), 121.5 (d, C-5), 93.5 (s, C-15), 82.2 (d, C-3), 81.8 (s, C-7), 80.9 (d, C-14), 73.9 (d, C-9), 68.3 (d, C-8), 46.9 (d, C-401 4), 42.0 (t, C-1), 39.4 (s, C-10), 38.6 (d, C-13), 37.8 (d, C-2), 23.2 (q, OAc-15), 23.2 (q, C-18), 21.2 (q, OAc-9), 21.2 (q, C-19), 21.1 (q, OAc-14), 20.3 (q, OAc-7), 20.2 (q, C-20), 17.6 (q, C-16), 16.5 (q, C-404 17); ESIMS m/z 665 $[\text{M} + \text{Na}]^+$, HRESIMS m/z 665.2932 $[\text{M} + \text{Na}]^+$, calcd for $\text{C}_{35}\text{H}_{46}\text{NaO}_{11}$, 665.2938.

406 **Reaction of Compound 4 with R- and S-MTPA Chlorides.**
407 Compound **4** (1.0 mg, 1.5 μmol) was treated with R-MTPA chloride
408 (30 μL) in 400 μL of dry pyridine overnight at room temperature. The
409 solvent was then removed to obtain the S-MTPA ester **4a** (1.2 mg,
410 93% yield). When compound **4** (1.0 mg, 1.5 μmol) was treated with S-
411 MTPA chloride, following the same procedure, 1.1 mg (87% yield) of
412 R-MTPA ester **4b** was obtained.

413 **S-MTPA Ester 4a.** Amorphous solid; ^1H NMR (CDCl_3) selected
414 values δ 5.77 (1H, dd, $J = 16.0, 7.9$ Hz, H-12), 5.66 (1H, d, $J = 10.0$
415 Hz, H-5), 5.21 (1H, bs, H-8), 5.20 (1H, bs, H-9), 5.13 (1H, bs, H-11),
416 5.10 (1H, bs, H-7), 5.02 (1H, d, $J = 2.6$ Hz, H-14), 2.60 (1H, m, H-
417 13). ESIMS (positive ion) m/z 859 $[\text{M} + \text{H}]^+$.

418 **R-MTPA Ester 4b.** Amorphous solid; ^1H NMR (CDCl_3) selected
419 values δ 5.75 (1H, dd, $J = 16.0, 7.9$ Hz, H-12), 5.67 (1H, d, $J = 10.0$ Hz,
420 H-5), 5.21 (1H, bs, H-8), 5.20 (1H, bs, H-9), 5.14 (1H, overlapped,
421 H-11), 5.13 (1H, bs, H-7), 5.00 (1H, bs, H-14), 2.59 (1H, m, H-13),
422 ESIMS m/z 859 $[\text{M} + \text{H}]^+$.

423 **Euphosquamosin B (5).** Colorless amorphous solid; $[\alpha]_D^{+25} +12.8$
424 (c 0.6, CHCl_3); ^1H NMR (CDCl_3 , 500 MHz) δ 7.94 (2H, d, $J = 7.4$
425 Hz, H-3' = H-7'), 7.54 (1H, t, $J = 7.4$ Hz, H-5'), 7.40 (2H, t, $J = 7.4$
426 Hz, H-4' = H-6'), 6.72 (1H, bs, H-5), 6.35 (1H, d, $J = 3.0$ Hz, H-3),
427 5.93 (1H, d, $J = 3.0$ Hz, H-14), 5.46 (1H, dd, $J = 16.5, 8.8$ Hz, H-12),
428 5.32 (1H, bs, H-8), 5.30 (1H, bs, H-9), 5.27 (1H, d, $J = 16.5$ Hz, H-
429 11), 4.72 (1H, d, $J = 4.4$ Hz, OH-7), 3.42 (1H, dd, $J = 6.6, 4.4$ Hz, H-
430 7), 2.58 (1H, m, H-13), 2.51 (2H, m, H-1), 2.19 (1H, overlapped, H-
431 2), 2.19 (3H, s, OAc-9), 2.10 (3H, s, OAc-14), 2.01 (3H, s, OAc-8),
432 1.58 (3H, s, OAc-15), 1.48 (3H, bs, H-17), 1.21 (3H, d, $J = 7.0$ Hz, H-
433 16), 0.99 (3H, s, H-18), 0.99 (3H, d, $J = 7.0$ Hz, H-20), 0.97 (3H, s,
434 H-19); ^{13}C NMR (CDCl_3 , 125 MHz) δ 173.6 (s, OAc-9), 171.1 (s,
435 OAc-15), 170.6 (s, OAc-14), 169.9 (s, OAc-8), 167.5 (s, C-1'), 138.2
436 (d, C-5), 138.0 (s, C-4), 137.9 (d, C-11), 133.4 (d, C-5'), 130.7 (d, C-
437 12), 130.3 (s, C-2'), 129.8 (d, C-3', C-7'), 128.6 (d, C-4', C-6'), 89.7
438 (s, C-15), 79.1 (d, C-3), 78.6 (d, C-7), 78.1 (s, C-6), 78.0 (d, C-14),
439 74.8 (d, C-9), 69.7 (d, C-8), 42.2 (t, C-1), 39.7 (s, C-10), 38.7 (d, C-
440 13), 37.1 (d, C-2), 29.9 (q, C-19), 29.1 (q, C-17), 22.6 (s, C-20), 22.5
441 (q, OAc-15), 22.4 (q, OAc-8), 21.4 (q, C-18), 21.3 (q, OAc-9), 21.3
442 (q, OAc-14), 14.1 (q, C-16), ESIMS m/z 681 $[\text{M} + \text{Na}]^+$, HRESIMS
443 m/z 681.2879 $[\text{M} + \text{Na}]^+$, calcd for $\text{C}_{35}\text{H}_{46}\text{NaO}_{12}$, 681.2881.

444 **Euphosquamosin C (6).** Colorless amorphous solid; $[\alpha]_D^{+25} -56$ (c
445 0.7, CHCl_3); ^1H NMR (CDCl_3 , 500 MHz) δ 7.94 (2H, d, $J = 7.4$ Hz,
446 H-3' = H-7'), 7.54 (1H, t, $J = 7.4$ Hz, H-5'), 7.42 (2H, t, $J = 7.4$ Hz, H-
447 4', H-6'), 6.02 (1H, d, $J = 3.0$ Hz, H-14), 6.02 (1H, d, $J = 15.5$ Hz, H-
448 11), 5.77 (1H, dd, $J = 15.5, 8.0$ Hz, H-12), 5.72 (1H, bs, H-5), 5.32
449 (1H, bd, $J = 7.2$ Hz, H-8), 4.63 (1H, overlapped, H-3), 4.60 (1H, bs,
450 H-17a), 4.39 (1H, bs, H-17b), 3.52 (1H, bd, $J = 4.5$ Hz, H-4), 2.76
451 (1H, m, H-2), 2.61 (1H, m, H-13), 2.58 (1H, overlapped, H-1), 2.56
452 (1H, m, H-7a), 2.26 (3H, s, OAc-14), 2.13 (3H, s, OAc-5), 2.08 (1H,
453 m, H-7b), 2.06 (3H, s, OAc-15), 1.99 (3H, s, OAc-8), 1.53 (1H,
454 overlapped, H-1), 1.35 (3H, s, H-18), 1.21 (3H, s, H-19), 1.02 (3H, d,
455 $J = 7.0$ Hz, H-20), 0.98 (3H, d, $J = 7.0$ Hz, H-16); ^{13}C NMR (CDCl_3 ,
456 125 MHz) δ 210.3 (s, C-9), 170.8 (s, OAc-8), 170.6 (s, OAc-14),
457 169.8 (s, OAc-15), 168.9 (s, OAc-5), 167.7 (s, C-3'), 139.2 (s, C-6),
458 135.4 (d, C-11), 133.4 (d, C-5'), 131.3 (d, C-12), 130.3 (s, C-2'),
459 129.8 (d, C-3', C-7'), 128.6 (d, C-4', C-6'), 115.8 (t, C-12), 87.9 (s, C-
460 15), 81.8 (d, C-3), 77.8 (d, C-14), 74.3 (s, C-8), 70.2 (d, C-5), 48.4
461 (s, C-10), 42.9 (d, C-4), 41.1 (t, C-1), 38.4 (d, C-13), 34.3 (t, C-7),

35.8 (d, C-2), 28.3 (q, C-19), 29.1 (q, C-17), 24.4 (q, C-18), 22.4 (s, 462
C-20), 22.2 (q, OAc-15), 21.4 (q, OAc-14), 21.3 (q, OAc-5), 20.6 (q, 463
OAc-8), 18.3 (q, C-16); ESIMS m/z 663 $[\text{M} + \text{Na}]^+$, HRESIMS m/z 464
663.2781 $[\text{M} + \text{Na}]^+$, calcd for $\text{C}_{35}\text{H}_{44}\text{NaO}_{11}$, 663.2776. 465

Yeast Strains and Growth Media. The yeast strains used in this 466
study are listed in Table 3. All strains were cultured in yeast extract- 467

Table 3. Yeast Strains Used in This Study

strain	genotype or description	source
AD1-8u ⁻	(<i>Mata</i> , <i>pdr1-3</i> , <i>ura3 his1</i> , $\Delta yor1::hisG$, $\Delta snq2::hisG$, $\Delta pdr5::hisG$, $\Delta pdr10::hisG$, $\Delta pdr11::hisG$, $\Delta ycf1::hisG$, $\Delta pdr3::hisG$, $\Delta pdr15::hisG$)	Nakamura et al., 2001 ³⁹
AD-CDR1	AD1-8u ⁻ cells harboring <i>CDR1</i> ORF integrated at <i>PDR5</i> locus	Nakamura et al., 2001 ³⁹
AD-MDR1	AD1-8u ⁻ cells harboring <i>MDR1</i> ORF integrated at <i>PDR5</i> locus	Pasrija et al., 2007 ⁷

peptone-dextrose (YEPD) broth (BIO101; Biomedical Life Systems, 468
Inc., Vista, CA, USA) at 30 °C. For agar plates, 2.5% (w/v) Bacto agar 469
(Difco, BD Biosciences, Franklin, NJ, USA) was added to the medium. 470
All strains were stored as frozen stocks with 15% glycerol at −80 °C. 471
Before each experiment, cells were freshly revived on YEPD plates 472
from the stock. 473

Reagents and Media. Chemicals such as fluconazole were 474
obtained from HiMedia (Mumbai, India). Agar medium was 475
purchased from Difco, BD Biosciences (Franklin Lakes, NJ, USA). 476
Nile Red and other molecular-grade chemicals were obtained from 477
Sigma Chemical Co. (St. Louis, MO, USA). All routine chemicals were 478
obtained from Qualigens (Mumbai, India) and were of analytical 479
grade. 480

Statistical Analysis. Data are the means \pm SD from duplicate 481
samples of at least three independent experiments. Differences 482
between the mean values were analyzed by Student's *t* test, and 483
results were considered significant when $p < 0.05$. 484

Transport Assays. Transport assays were done by monitoring Nile 485
Red (NR) accumulation. The accumulation of NR in cells over- 486
expressing Cdr1p (AD-CDR1) or Mdr1p (AD-MDR1) was measured 487
by flow cytometry with a FACSort flow cytometer (Becton-Dickinson 488
Immunocytometry Systems). Briefly, cells with an OD₆₀₀ of 0.1 were 489
inoculated and allowed to grow at 30 °C with shaking, until the OD₆₀₀ 490
reached 0.25. The cells were then harvested and resuspended as a 5% 491
cell suspension in diluted medium (containing one part of YEPD and 492
two parts of water). NR was added to a final concentration of 7 μM , 493
and the cells were incubated at 30 °C for 30 min in the absence or 494
presence of each inhibitor at a concentration 10-fold higher than 495
substrate (70 μM). The cells were then harvested, and 10 000 cells 496
were analyzed in the acquisition. The analysis was performed using the 497
CellQuest software (Becton Dickinson Immunocytometry Systems). 498

Cytotoxicity and Sensitization to Fluconazole. Yeast cells 499
(10⁴) were seeded into 96-well plates in either absence or presence of 500
varying concentrations of inhibitors (0.15–80 μM) and were grown 501
for 48 h at 30 °C. The IC₅₀ values of cytotoxicity were determined by 502
measuring the optical density of each strain. Growth in the absence of 503
any inhibitor was considered as 100%, and the concentration 504
producing 50% growth was taken as the IC₅₀ value; the resistance 505
index (RI) was calculated as the ratio between the IC₅₀ values 506
determined for the strain overexpressing either Cdr1p (AD-CDR1) or 507
Mdr1p (AD-MDR1) relative to that of the control strain (AD1-8u⁻). 508
The interaction of the respective inhibitors with FLC was evaluated by 509
the checkerboard method recommended by the CLSI (formerly 510
NCCLS), and was expressed as the fractional inhibitory concentration 511
index (FICI). Ranges of concentrations were used: 0.15–800 μM for 512
fluconazole, and 0.15–80 μM of respective inhibitors. FICI values 513
were calculated as the sum of the FICs of each agent (FLC and 514
inhibitors). The FIC of each agent was calculated as the MIC of the 515
agent in combination divided by the MIC of the agent alone.⁹ 516

■ ASSOCIATED CONTENT

● Supporting Information

¹H and HSQC NMR spectra for euphosquamosins A–C (4–6). This material is available free of charge via the Internet at <http://pubs.acs.org>.

■ AUTHOR INFORMATION

Corresponding Authors

*(O.T.-S.) E-mail: scatagli@unina.it. Tel: +39-081678509. Fax: +39-081678552.

*(A.D.P.) E-mail: a.dipietro@ibcp.fr. Tel: +33-472722629. Fax: +33-47272 2604.

Author Contributions

⊗ Both senior investigators contributed equally to the work supervision.

Notes

The authors declare no competing financial interest.

■ ACKNOWLEDGMENTS

Indian financial support was provided by Grants to R.P. from the Department of Biotechnology (BT/01/CEIB/10/III/02). M.K.R. acknowledges funding from a UGC Dr. D.S. Kothari Postdoctoral Fellowship. French financial support was provided to A.D.P. by the CNRS and University of Lyon (UMR 5086), the Ligue Nationale Contre le Cancer (Equipe labellisée Ligue 2014), and an international ANR grant (2010-INT-1101-01). We are grateful to Isfahan University of Medical Sciences for a 6-month fellowship for Y.S. at the Università del Piemonte Orientale, and to Mr. Bahram Zehzad for identification of the plant material.

■ REFERENCES

- (1) Richardson, M. D. *J. Antimicrob. Chemother.* **2005**, *56*, iS–i11.
- (2) Pfaller, M. A.; Boyken, L.; Hollis, R. J.; Kroeger, J.; Messer, S. A.; Tendolkar, S.; Diekema, D. J. *J. Clin. Microbiol.* **2007**, *46*, 150–156.
- (3) Perlin, D. S. *Future Microbiol.* **2011**, *6*, 441–457.
- (4) White, T. C.; Marr, K. A.; Bowden, R. A. *Clin. Microbiol. Rev.* **1998**, *11*, 382–402.
- (5) Prasad, R.; De Worgifosse, P.; Goffeau, A.; Balzi, E. *Curr. Genet.* **1995**, *27*, 320–329.
- (6) Sanglard, D.; Ischer, F.; Monod, M.; Bille, J. *Microbiology* **1997**, *143*, 405–416.
- (7) Pasrija, R.; Banerjee, D.; Prasad, R. *Eukaryot. Cell* **2007**, *6*, 443–453.
- (8) Prasad, R.; Panwar, S. L.; Smriti. *Adv. Microb. Physiol.* **2002**, *46*, 155–201.
- (9) Niimi, K.; Harding, D. R.; Parshot, R.; King, A.; Lun, D. J.; Decottignies, A.; Niimi, M.; Lin, S.; Cannon, R. D.; Goffeau, A.; Monk, B. C. *Antimicrob. Agents Chemother.* **2004**, *48*, 1256–1271.
- (10) Hiraga, K.; Yamamoto, S.; Fukuda, H.; Hamanaka, N.; Oda, K. *Biochem. Biophys. Res. Commun.* **2005**, *328*, 1119–1125.
- (11) Tanabe, K.; Lamping, E.; Adachi, K.; Takano, Y.; Kawabata, K.; Shizuri, Y.; Niimi, M.; Uehara, Y. *Biochem. Biophys. Res. Commun.* **2007**, *364*, 990–995.
- (12) Lamping, E.; Monk, B. C.; Niimi, K.; Holmes, A. R.; Tsao, S.; Tanabe, K.; Niimi, M.; Uehara, Y.; Cannon, R. D. *Eukaryot. Cell* **2007**, *6*, 1150–1165.
- (13) Prasad, R.; Sharma, M.; Rawal, M. K. *J. Amino Acids* **2011**, No. 531412, DOI: 10.4061/2011/531412.
- (14) Silva, L. V.; Sanguinetti, M.; Vandeputte, P.; Torelli, R.; Rochat, B.; Sanglard, D. *Antimicrob. Agents Chemother.* **2013**, *57*, 873–886.
- (15) Shukla, S.; Sauna, Z. E.; Prasad, R.; Ambudkar, S. V. *Biochem. Biophys. Res. Commun.* **2004**, *322*, 520–525.

- (16) Sharma, M.; Manoharlal, R.; Shukla, S.; Puri, N.; Prasad, T.; Ambudkar, S. V.; Prasad, R. *Antimicrob. Agents Chemother.* **2009**, *53*, 3256–3265.
- (17) Sharma, M.; Prasad, R. *Antimicrob. Agents Chemother.* **2011**, *55*, 4834–4843.
- (18) Appendino, G.; Della Porta, C.; Conseil, G.; Sterner, O.; Mercalli, E.; Dumontet, C.; Di Pietro, A. *J. Nat. Prod.* **2003**, *66*, 140–142.
- (19) Jiao, W.; Dong, W.; Deng, M.; Lu, R. *Bioorg. Med. Chem.* **2009**, *17*, 4786–4792.
- (20) Duarte, N.; Varga, A.; Cherepnev, G.; Radics, R.; Molnar, J.; Ferreira, M. J. *Bioorg. Med. Chem.* **2007**, *15*, 546–554.
- (21) Corea, G.; Fattorusso, E.; Lanzotti, V.; Tagliatela-Scafati, O.; Appendino, G.; Simon, P.-N.; Dumontet, C.; Di Pietro, A. *J. Med. Chem.* **2003**, *46*, 3395–3402.
- (22) Corea, G.; Fattorusso, E.; Lanzotti, V.; Motti, R.; Simon, P.-N.; Dumontet, C.; Di Pietro, A. *J. Med. Chem.* **2004**, *47*, 988–992.
- (23) Vasas, A.; Sulyok, E.; Rédei, D.; Forgo, P.; Szabo, P.; Zupko, P.; Berenyi, A.; Molnar, J.; Hohmann, J. *J. Nat. Prod.* **2011**, *74*, 1453–1461.
- (24) Barile, E.; Borriello, M.; Di Pietro, A.; Doreau, A.; Fattorusso, C.; Fattorusso, E.; Lanzotti, V. *Org. Biomol. Chem.* **2008**, *6*, 1756–1762.
- (25) Corea, G.; Di Pietro, A.; Dumontet, C.; Fattorusso, E.; Lanzotti, V. *Phytochem. Rev.* **2009**, *8*, 431–447.
- (26) Ferreira, R. J.; dos Santos, D. J.; Ferreira, M. J.; Guedes, R. C. *J. Chem. Inf. Model.* **2011**, *51*, 1315–1324.
- (27) Ahmed, A. A.; Gherraf, N.; El-Bassuony, A. A.; Rhouati, S.; Gad, M. H.; Ohta, S.; Hirata, T. *Nat. Prod. Commun.* **2006**, *1*, 273–279.
- (28) Hohmann, J.; Molnar, J.; Redei, D.; Evanics, F.; Forgo, P.; Kalman, A.; Argay, G.; Szabo, P. *J. Med. Chem.* **2002**, *45*, 2425–2431.
- (29) Yamamura, S.; Shizuri, S.; Kosemura, S.; Ohtsuka, J.; Tayama, T.; Ohba, S.; Ito, M.; Saito, Y.; Terada, Y. *Phytochemistry* **1989**, *28*, 3421–3436.
- (30) Shokoohinia, Y.; Chianese, G.; Zolfaghari, B.; Sajjadi, S.-E.; Appendino, G.; Tagliatela-Scafati, O. *Fitoterapia* **2011**, *82*, 317–322.
- (31) Ohtani, I.; Kusumi, T.; Kashman, Y.; Kakisawa, H. *J. Am. Chem. Soc.* **1991**, *113*, 4092–4096.
- (32) Valdameri, G.; Pereira Rangel, L.; Sapatafora, C.; Guitton, J.; Gauthier, C.; Arnaud, O.; Ferreira-Pereira, A.; Falson, P.; Winnischofer, S. M. B.; Rocha, M. E. M.; Tringali, C.; Di Pietro, A. *ACS Chem. Biol.* **2012**, *7*, 322–330.
- (33) Holmes, A. R.; Kenija, M. V.; Ivnitski-Steele, I.; Monk, B. C.; Lamping, E.; Sklar, L. A.; Cannon, R. D. *Antimicrob. Agents Chemother.* **2012**, *56*, 1508–1515.
- (34) Conseil, G.; Pérez-Victoria, J. M.; Jault, J. M.; Gamarro, F.; Goffeau, A.; Hofmann, J.; Di Pietro, A. *Biochemistry* **2001**, *40*, 2564–2471.
- (35) Conseil, G.; Pérez-Victoria, J. M.; Renoir, J. M.; Goffeau, A.; Di Pietro, A. *Biochim. Biophys. Acta* **2003**, *1614*, 131–134.
- (36) Perez-Victoria, F. J.; Conseil, G.; Munoz-Fernandez, F.; Perez-Victoria, J. M.; Dayan, G.; Marsaud, V.; Castans, S.; Gamarro, F.; Renoir, J. M.; Di Pietro, A. *Cell. Mol. Life Sci.* **2003**, *60*, 526–535.
- (37) Kolaczowski, M.; van der Rest, M.; Cybularz-Lolaczowska, A.; Soumillion, J.-P.; Konings, W. N.; Goffeau, A. *J. Biol. Chem.* **1996**, *271*, 31543–31548.
- (38) Rogers, B.; Decottignies, A.; Kolaczowski, M.; Carvajal, E.; Balzi, E.; Goffeau, A. *J. Mol. Microbiol. Biotechnol.* **2001**, *3*, 207–214.
- (39) Nakamura, K.; Niimi, M.; Niimi, K.; Holmes, A. R.; Yates, J. E.; Decottignies, A.; Monk, B. C.; Goffeau, A.; Cannon, R. D. *Antimicrob. Agents Chemother.* **2001**, *45*, 3366–3374.